Dual Roles of Glutathione in Ecdysone Biosynthesis and Antioxidant Function During Larval Development in *Drosophila*

Sora Enya,*,[1,2] Chikana Yamamoto,*,[2] Hajime Mizuno,†,[3] Tsuyoshi Esaki,†,[4] Hsin-Kuang Lin,* Masatoshi Iga,‡,[5] Kana Morohashi,* Yota Hirano,* Hiroshi Kataoka,‡ Tsutomu Masujima,† Yuko Shimada-Niwa,§,[6] and Ryusuke Niwa,††,[6]**

*Graduate School of Life and Environmental Sciences and **Faculty of Life and Environmental Sciences, University of Tsukuba, Ibaraki 305-8572, Japan, †Laboratory of Single-Cell Mass Spectrometry, The Institute of Physical and Chemical Research (RIKEN) Quantitative Biology Center, Suita, Osaka 565-0874, Japan, ‡Graduate School of Frontier Sciences, The University of Tokyo, Kashiwa, Chiba 277-8562, Japan, §Life Science Center of Tsukuba Advanced Research Alliance, University of Tsukuba, Ibaraki 305-8577, Japan, and ††Precursory Research for Embryonic Science and Technology, Japan Science and Technology Agency, Kawaguchi, Saitama 332-0012, Japan

ORCID IDs: 0000-0001-5757-4329 (Y.S.-N.); 0000-0002-1716-455X (R.N.)

ABSTRACT Ecdysteroids, including the biologically active hormone 20-hydroxyecdysone (20E), play essential roles in controlling many developmental and physiological events in insects. Ecdysteroid biosynthesis is achieved by a series of specialized enzymes encoded by the Halloween genes. Recently, a new class of Halloween gene, *noppera-bo* (*nobo*), encoding a glutathione *S*-transferase (GST) in dipteran and lepidopteran species, has been identified and characterized. GSTs are well known to conjugate substrates with the reduced form of glutathione (GSH), a bioactive tripeptide composed of glutamate, cysteine, and glycine. We hypothesized that GSH itself is required for ecdysteroid biosynthesis. However, the role of GSH in steroid hormone biosynthesis has not been examined in any organisms. Here, we report phenotypic analysis of a complete loss-of-function mutant in the γ-*glutamylcysteine synthetase catalytic subunit* (*Gclc*) gene in the fruit fly *Drosophila melanogaster*. *Gclc* encodes the evolutionarily conserved catalytic component of the enzyme that conjugates glutamate and cysteine in the GSH biosynthesis pathway. Complete *Gclc* loss-of-function leads to drastic GSH deficiency in the larval body fluid. *Gclc* mutant animals show a larval-arrest phenotype. Ecdysteroid titer in *Gclc* mutant larvae decreases, and the larval-arrest phenotype is rescued by oral administration of 20E or cholesterol. Moreover, *Gclc* mutant animals exhibit abnormal lipid deposition in the prothoracic gland, a steroidogenic organ during larval development. All of these phenotypes are reminiscent to *nobo* loss-of-function animals. On the other hand, *Gclc* mutant larvae also exhibit a significant reduction in antioxidant capacity. Consistent with this phenotype, *Gclc* mutant larvae are more sensitive to oxidative stress response as compared to wild-type. Nevertheless, the ecdysteroid biosynthesis defect in *Gclc* mutant animals is not associated with loss of antioxidant function. Our data raise the unexpected hypothesis that a primary role of GSH in early *D. melanogaster* larval development is ecdysteroid biosynthesis, independent from the antioxidant role of GSH.

KEYWORDS glutathione; Gclc; ecdysteroid; antioxidant; *Drosophila melanogaster*

ECDYSTEROIDS are principal insect steroid hormones, playing versatile roles in the regulation of many developmental and physiological processes, especially molting and metamorphosis (Yamanaka *et al.* 2013; R. Niwa and Y. S. Niwa 2014; Y. S. Niwa and R. Niwa 2014, 2016; Uryu *et al.* 2015). Ecdysteroids, including ecdysone and 20-hydroxyecdysone (20E), are synthesized from dietary cholesterol or phytosterols via a series of hydroxylation and oxidation steps. Over the past 15 years, a number of enzyme genes that are responsible for ecdysteroid biosynthesis have been identified and characterized, some of which are often called the Halloween genes (Gilbert 2004; Rewitz *et al.* 2006). The Halloween genes include *noppera-bo* (Chanut-Delalande *et al.* 2014; Enya *et al.* 2014), *shroud* (Niwa *et al.* 2010), *spook* (Namiki *et al.* 2005; Ono *et al.* 2006), *phantom* (Niwa *et al.* 2004; Warren *et al.* 2004), *disembodied* (Chávez *et al.* 2000; Warren *et al.* 2002), *shadow* (Warren *et al.* 2002), and *shade* (Petryk *et al.* 2003). The Halloween genes are characterized by typical phenotypes of their null mutants in the fruit fly *Drosophila melanogaster*, which display embryonic lethality, abnormalities in embryonic cuticle

differentiation, and deficiencies in ecdysteroid levels (Nüsslein-Volhard *et al.* 1984; Chávez *et al.* 2000). Among them, *phantom*, *disembodied*, *shadow*, and *shade* encode cytochrome P450 monooxygenases, each of which has been biochemically characterized as enzymes essential for catalyzing a particular step of the ecdysteroid biosynthesis pathway (R. Niwa and Y. S. Niwa 2014).

Another Halloween gene, *noppera-bo* (*nobo*), belongs to a cytosolic glutathione *S*-transferase (GST) ε family and is well conserved, at least in dipteran and lepidopteran species (Chanut-Delalande *et al.* 2014; Enya *et al.* 2014, 2015). *Nobo* genes are synonymous with *D. melanogaster GSTe14*, *Anopheles gambiae GSTe8*, and *Bombyx mori GSTe7*. *Nobo* is predominantly expressed in tissues biosynthesizing ecdysteroids, including the prothoracic gland (PG) and the ovary. Notably, the *nobo* loss-of-function phenotype in *D. melanogaster* is well rescued by oral administration of cholesterol, the most upstream precursor of the ecdysteroid biosynthesis pathway (Chanut-Delalande *et al.* 2014; Enya *et al.* 2014). Therefore, Nobo seems not to catalyze any particular ecdysteroidal intermediates, but rather to regulate the transport and/or metabolism of cholesterol through unknown mechanisms.

The well-investigated reaction catalyzed by GSTs is the addition of the reduced form of L-γ-glutamyl-L-cysteinylglycine, or glutathione (GSH), to substrates. Although endogenous substrate(s) for Nobo have not yet been identified, we demonstrated that a recombinant *D. melanogaster* Nobo protein possesses the ability to catalyze the conjugation of reduced GSH to an artificial substrate (Fujikawa *et al.* 2015). It is noteworthy that the mammalian GSTA3-3 is also involved in steroid hormone biosynthesis (Raffalli-Mathieu and Mannervik 2005; Fedulova *et al.* 2010), while *GSTA3-3* is not orthologous to *nobo*. Therefore, it is feasible to hypothesize that GSH itself is commonly required for steroid hormone biosynthesis across species, although this hypothesis has not yet been examined in any organisms.

GSH is biosynthesized *de novo* by the consecutive action of two enzymes to conjugate L-glutamine, L-cysteine, and glycine. The first enzyme is glutamate–cysteine ligase (GCL, EC 6.3.2.2), also known as γ-glutamylcysteine synthase, which generates γ-glutamylcysteine (Figure 1A). GCL is a heterodimer of a catalytic subunit (GCLc) and a modulatory subunit (GCLm), which are encoded by different genes (Griffith and Mulcahy 1999; Lu 2014). The GCLc subunit can catalyze the formation of γ-glutamylcysteine in the absence of GCLm, but its activity is increased substantially by covalent interactions with GCLm (Sies 1999; Lu 2014). The second enzyme required for *de novo* GSH biosynthesis is GSH synthase (GS, EC 6.3.2.3), which links glycine to γ-glutamylcysteine to form GSH (Figure 1A) (Lu 2014). It is generally thought that GCL, but not GS, is the rate-limiting enzyme in GSH biosynthesis (Lu 2014).

In *D. melanogaster*, the *Gclc* and *Gclm* genes have been reported and their products have been enzymatically characterized (Fraser *et al.* 2002, 2003). Moreover, *Gclc* overexpression exerts a beneficial effect on survival under normal and oxidative stress conditions in *D. melanogaster* (Orr *et al.* 2005; Luchak *et al.* 2007; Radyuk *et al.* 2012; Moskalev *et al.* 2016). Conversely, *Gclc* RNA interference (RNAi) animals exhibit neuronal defects, greater sensitivity to oxidative stress, and eventually reduced survival (Luchak *et al.* 2007; Mercer *et al.* 2016). All of these studies support the idea that GSH is a major antioxidant in the cell and is critical for protecting cells against reactive oxygen species in adult flies.

In contrast, the role of GSH during *D. melanogaster* development has not been extensively studied to date; a single genetic study has reported that a mutant animal that lacks a large fragment of the 5′ untranslated region of *Gclc* is developmentally lethal (Luchak *et al.* 2007). Therefore, the main objective of this study is to investigate the role of *Gclc* during development using a *Gclc* null mutant allele, and to examine whether GSH is involved in ecdysteroid biosynthesis and ecdysteroid-dependent developmental processes in *D. melanogaster*.

Materials and Methods

Fly strains

D. melanogaster flies were reared on standard agar–cornmeal medium (standard food) at 25° under a 12/12 hr light/dark cycle. w^{1118} was used as the wild-type (control) strain. *UAS-Gclc#3* and *UAS-Gclc#6* transgenic strains (Orr *et al.* 2005) were kindly gifted from William C. Orr (Southern Methodist University). *phm-GAL4#22* (McBrayer *et al.* 2007) and *DMef2-GAL4* (Ranganayakulu *et al.* 1996) were also kind gifts from Michael B. O'Connor (University of Minnesota) and Eric N. Olson (University of Texas Southwestern Medical Center at Dallas), respectively. *ppl-GAL4* (Colombani *et al.* 2003) and *byn-GAL4* (Iwaki and Lengyel 2002) were obtained from Hiroko Sano (Kurume University, Japan) and Ryutaro Murakami (Yamaguchi University, Japan), respectively. *arm-GAL4* (Loncle *et al.* 2007), *elav-GAL4* (Luo *et al.* 1994), *tubP-GAL4* (Lee and Luo 1999), *UAS-dicer2* (#24650), and *hsFLP ovoD FRT19A* (#23880) were provided by the Bloomington *Drosophila* Stock Center. *p{GawB}NP3084* (Nehme *et al.* 2007) was provided by the Kyoto Stock Center. *UAS-nobo-IR* (#101884KK and #40316GD) and *UAS-Gclc-IR* (#108022KK and #33512GD) were obtained from

doi: https://doi.org/10.1534/genetics.117.300391
Manuscript received March 28, 2017; accepted for publication October 8, 2017; published Early Online October 11, 2017.
Available freely online through the author-supported open access option.
Supplemental material is available online at www.genetics.org/lookup/suppl/doi:10.1534/genetics.117.300391/-/DC1.
This article is dedicated to Tsutomu Masujima, who died during the course of the study.
[1]Present address: Advanced Telecommunications Research Institute International/The TNS BioMEC-X Laboratories, Hikaridai Seika-cho 2-2-2, Sorakugun, Kyoto 619-0288, Japan.
[2]These authors contributed equally to this work.
[3]Present address: School of Pharmaceutical Sciences, University of Shizuoka, Yada 52-1, Suruga-ku, Shizuoka 422-8526, Japan.
[4]Present address: Laboratory of Bioinformatics, National Institutes of Biomedical Innovation, Health and Nutrition, Saito-Asagi 7-6-8, Ibaraki, Osaka 567-0085, Japan.
[5]Present address: Institute of Agrobiological Sciences, National Agriculture and Food Research Organization, Owashi 2-1, Tsukuba, Ibaraki 305-8634, Japan.
[6]Corresponding authors: University of Tsukuba, Tennoudai 1-1-1, Tsukuba, Ibaraki 305-8572, Japan. E-mails: shimada.yuko.gn@u.tsukuba.ac.jp; ryusuke-niwa@umin.ac.jp.

the Vienna *Drosophila* RNAi center. *y*^{1} *v*^{1} *nos-phiC31*; *attP40* and *y*^{2} *cho*^{2} *v*^{1}; *attP40*{*nos-Cas9*}/*CyO* (Kondo and Ueda 2013) were obtained from the National Institute of Genetics, Japan.

Generation of Gclc loss-of-function mutant allele

Generation of the *Gclc* allele was carried out by the clustered regularly interspaced short palindromic repeats (CRISPR)/Cas9 system using the pBFv-U6.2 vector (Kondo and Ueda 2013) provided by the National Institute of Genetics, Japan. To minimize off-target effects of CRISPR/Cas9, we confirmed by BLAST search that no 15-nucleotide stretches within the selected target sequence (23 nucleotides including the protospacer adjacent motif) matched any other sequence on the X chromosome. Sense and antisense oligonucleotides corresponding to single guide RNA (sgRNA) target sequences (5′-CTTCGTTCGACGATGAACAGAAGG-3′ and 5′-AAACCCTTCTGTTCATCGTCGAAC-3′, respectively) were annealed. The annealed oligonucleotide fragment was inserted into a *Bbs*I-digested pBFv-U6.2 vector. The *Gclc* sgRNA vector was injected into embryos of the *y*^{1} *v*^{1} *nos-phiC31*; *attP40* strain, generating the *U6-Gclc-sgRNA* strain. *Nos-Cas9*-based gene targeting was carried out as previously described (Kondo and Ueda 2013). Males carrying both *nos-Cas9* and *U6-Gclc-sgRNA* transgenes were crossed to *FM7c Bar* balancer flies by mass mating. Single females from their progeny carrying *FM7c Bar* were crossed with *FM7c Bar/Y* males, establishing independent isogenized strains. Among them, we surveyed strains that showed male hemizygous lethality. To confirm indel mutations at the *Gclc* locus in each hemizygous lethal strain, we performed the T7EI assay as previously described (Kondo and Ueda 2013). Briefly, the DNA fragment including the *Cas9* target site was amplified by PCR with KOD FX Neo (Toyobo, Osaka, Japan), the extracted genome DNA from each strain, and the primers (5′-GGGTGACATATT GAAATGGGGCG-3′ and 5′-CCAGATTGAAGTGTGCCATCA GACC-3′, shown as primerF and primerR in Figure 1B, respectively). The PCR products were treated with T7 endonuclease (New England Biolabs, Beverly, MA). The reacted samples were analyzed by agarose gel electrophoresis. After these procedures, we eventually selected the *Gclc*^{46} allele. Since this allele has a large (46 bp) deletion in the coding sequence, we determined that the PCR product size difference between *Gclc*^{WT} and *Gclc*^{46} was easily detected without T7 endonuclease treatment (Figure 1C). The PCR product from the *Gclc*^{46} allele was subcloned into a *Sma*I-digested pBluescript II SK(-) plasmid (Promega, Madison, WI), then sequenced with T3 and T7 primers. The *Gclc*^{46} strain was backcrossed with the *w*^{1118} control strain five times and then balanced with the *FM7 act-GFP* balancer. We used this backcrossed strain—*w*^{1118} *Gclc*^{46}—to which we refer throughout as "*Gclc*^{46}," for all experiments in this study. We also generated *Gclc*^{46} *FRT19Aneo/FM7 act-GFP* for germline clone analysis.

Mass-spectrometric quantification of glutathione

Larval bodies of control (*w*^{1118}) and *Gclc*^{46}/*Y* second-instar larvae [60 hr after egg laying (AEL)] were severed on parafilm. The body fluid (0.2 μl) that oozed from the five severed larvae was collected, then mixed with 1 μl distilled water containing 1 mM 2-mercaptoethanol (Nacalai Tesque, Kyoto, Japan). Due to the presence of 2-mercaptoethanol, glutathione disulfide (GSSG) in the sample is converted to GSH. Body-fluid proteins were removed by centrifugation at 10,000 × *g* for 5 min at 4° after being mixed with 1.5 μl of 0.1% formic acid (Honeywell Fluka, Morristown, NJ) in 80% methanol (Kanto Chemical, Tokyo, Japan). One microliter of the supernatant was introduced to a nanospray tip (Cellomics Tip CH-1; HUMANIX, Hiroshima, Japan), which was then set on a nano-electrospray ionization ion source. Mass-spectrometric detection of GSH was performed on a high-resolution mass spectrometer (LTQ Orbitrap Velos Pro; Thermo Fisher Scientific, Waltham, MA) as previously described (Fujii *et al.* 2015). The spray voltage for positive-ion detection mode was 1000 V. GSH detection was mainly performed in the range of *m/z* 100–1000. The spectrometer was calibrated by polytyrosine (CS Bio, Menlo Park, CA) prior to the experiments. Data analysis was conducted using Xcalibur software (Thermo Fisher Scientific). Target mass peaks were detected in the ± 5 ppm range, relative to the theoretical mass of GSH (*m/z* 308.091).

Mass-spectrometric quantification of 20E

For the measurement of 20E in whole bodies of control (*w*^{1118}/*Y*) and *w*^{1118} *Gclc*^{46}/*Y* hemizygous animals, second-instar larvae (50 hr AEL) of each genotype were collected and the wet weight of each sample was measured. The samples were frozen with liquid nitrogen and stored at −80° until measurement. Extraction of steroids, HPLC fractionation, and mass-spectrometric analyses were performed as previously described (Igarashi *et al.* 2011; Hikiba *et al.* 2013). In the mass-spectrometric analyses, the exact quantification range was 0.49–31.25 ng/ml. In this experimental condition, the limit of quantification of 20E was 3.68 pg of 20E/mg of wet weight sample.

Scoring of developmental progression of Gclc mutant animals

Gclc^{46}/*FM7 act-GFP* and *w*^{1118} females were crossed with *FM7 act-GFP/Y* males, respectively. Eggs were laid on grape plates with yeast pastes at 25° for 4 hr. Twenty-four hours AEL, *GFP*-negative first-instar larvae, which correspond to *Gclc*^{46}/*Y* and *w*^{1118}/*Y* males, were collected under a fluorescence dissection microscope M165FC (Leica, Wetzlar, Germany). Sixty hatched *GFP*-negative first-instar larvae were transferred into vials with standard food (30 animals per vial) and kept at 25°. Every 24 hr, developmental stages were scored by tracheal morphology as previously described (Niwa *et al.* 2010).

Feeding rescue experiments with various chemicals

Two grams of standard food was kneaded with 200 μl of the following chemical solutions: 50 mg/ml cholesterol (Sigma [Sigma Chemical], St. Louis, MO) in 100% ethanol, 50 mg/ml 20E (ENZO Life Sciences, Farmingdale, NY) in 100% ethanol, 10 mg/ml L(+)-ascorbic acid in distilled water, and 50–200 mg/ml reduced form of GSH (Nacalai

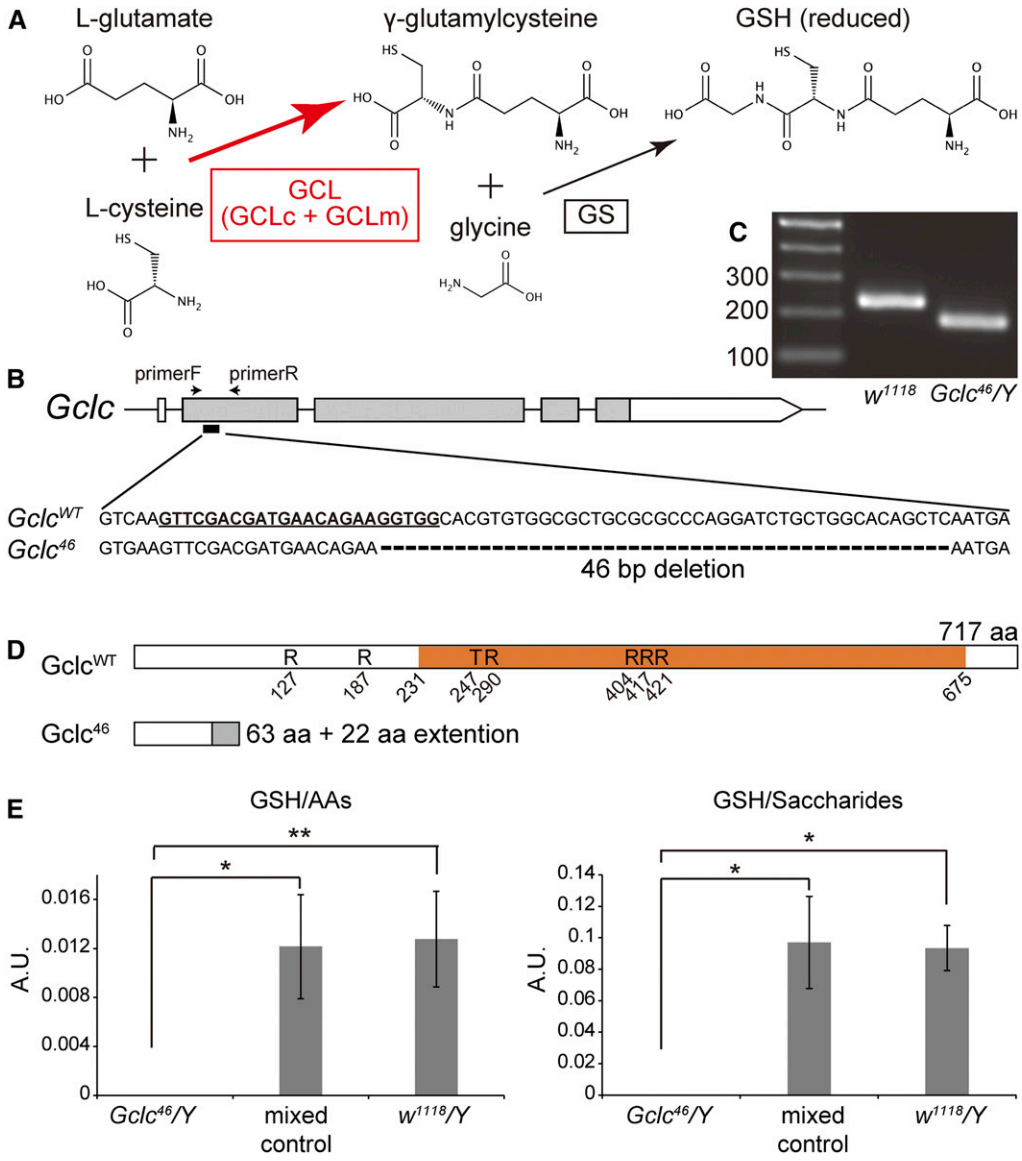

Figure 1 *Gclc* is required for glutathione (GSH) biosynthesis. (A) Schematic representation of the glutathione biosynthesis pathway. GCL, γ-glutamylcysteine ligase; GCLc, catalytic subunit of GCL; GCLm, modifier subunit of GCL; and GS, glutathione synthetase. (B) The genomic structures of wild-type *Gclc* ($Gclc^{WT}$) and the $Gclc^{46}$ allele. The boxes and lines indicate the exons and introns of *Gclc*, respectively, based on the description in FlyBase (http://flybase.org/reports/FBgn0040319.html). The $Gclc^{46}$ allele lacks 46 bp in the second exon. The gray and white colors indicate the coding sequence region and untranslated regions, respectively. Bold underlined characters indicate single guide RNA target and protospacer adjacent motif sequences. (C) Genomic PCR of control (w^{1118}) and $Gclc^{46}/Y$ first-instar larvae. Control larvae were a mixture of both males and females. The PCR primers used are shown in (B). 100, 200, and 300-bp size markers are displayed in the left lane. The PCR products of $Gclc^{WT}$ and $Gclc^{46}$ alleles are 236 and 190 bp, respectively. (D) The predicted primary structures of the proteins encoded by the $Gclc^{WT}$ and $Gclc^{46}$ genes. The orange box indicates the catalytic domain (231–675 aa) classified as γ-glutamylcysteine synthetase/glutamine synthetase clan (http://pfam.xfam.org/clan/CL0286) by Pfam (Finn *et al.* 2016). The $Gclc^{46}$ gene product is thought to contain the first 63 aa of the wild-type GCLc protein fused with an additional 22-aa extension (gray), which shows no obvious homology to any known protein. The 85-aa protein lacks equivalent amino acid residues that are identified as substrate-binding determinants of GCLc in other organisms, including R127 of the human GCLc (Hamilton *et al.* 2003) and others of *Trypanosoma brucei* GCLc (Abbott *et al.* 2002). (E) GSH amounts in hemolymph from control and $Gclc^{46}/Y$ larvae at the second-instar stage, when $Gclc^{46}/Y$ showed developmental-arrest phenotype, as shown in Figure 2. w^{1118}/Y male larvae and a mixed population of larvae of $Gclc^{46}$/*FM7 actin-GFP*, *FM7 act-GFP*/*Y*, and homozygous *FM7 actin-GFP* (mixed control) were used as control. The arbitrary units (A.U.) were normalized by total amounts of amino acids (AAs) (left) and of saccharides (right) that were simultaneously measured in hemolymph samples. Each bar represents the mean ± SEM. $N = 3$. * $P < 0.05$ and ** $P < 0.01$ by Student's *t*-test.

Tesque) in distilled water containing 1 mg/ml L(+)-ascorbic acid. For feeding experiments using ethacrynic acid (EA), standard food was kneaded with 0.01, 0.05, 0.1, 0.2, and 0.5% EA (Tokyo Kasei Kogyo, Tokyo, Japan) at final concentrations. First-instar larvae of $Gclc^{46}/Y$ and w^{1118}/Y were collected as described above (see *Scoring of developmental progression of Gclc mutant animals*). The larvae were then transferred into vials with standard food supplemented with chemicals. Each vial contained a maximum of 30 animals. Animals were reared at 25°C and continuously fed the supplemented food throughout larval development. Developmental stages of larvae were scored by tracheal morphology.

Low-sterol food assay

A recipe for Low-sterol food (LSF) was based on Carvalho *et al.* (2010) with some modifications. LSF used in this study was a mixture of 10% yeast autolysate (Sigma), 10% glucose, 1% purified agar, 0.3% propionic acid, and 0.06% butyl p-hydroxybenzoate (all Nacalai Tesque). Cholesterol-supplemented LSF was prepared by adding cholesterol (Wako, Osaka, Japan) to LSF. The final concentration of cholesterol in this food was 6.2 μg/ml. In the original recipe of Eaton's group, yeast autolysate and agarose for the lipid-depleted medium were chloroform-extracted (Carvalho *et al.* 2010). However, we found that even when we did not treat these

materials with chloroform, the control larvae on LSF exhibited a reproducible larval-arrest phenotype (Figure 4A). More importantly, the larval-arrest phenotype on LSF was restored by adding cholesterol to LSF (Figure 4A), implying that sterol contents in our LSF were significantly reduced. We should note that the phenotype on our LSF was weaker than the phenotype on Eaton's lipid-depleted medium (Carvalho *et al.* 2010), probably because our LSF recipe omitted the chloroform extraction procedure.

Nile red staining and quantification

Dissection of the brain-ring gland complex was performed as described in Imura *et al.* (2017). The brain-ring gland complexes were dissected from second-instar larvae at 60 hr AEL in phosphate-buffered saline (PBS), then fixed in 4% paraformaldehyde for 1 hr at room temperature. Fixed tissues were washed three times with PBS for 10 min and incubated in 1 μg/ml Nile Red (Wako) solution dissolved in PBS + 0.5% Tween 20 (PBST) for 30 min at room temperature. Incubated tissues were then washed three times with 0.3% PBST for 10 min and mounted using VECTASHIELD mounting medium (Vector Laboratories, Burlingame, CA). Confocal images were captured using a LSM 700 laser scanning microscope (Zeiss [Carl Zeiss], Thornwood, NY). Images of fluorescence intensity were analyzed using ImageJ (Schneider *et al.* 2012).

Evaluation of antioxidant capacity

For the quantitative determination of the antioxidant capacity of larval body fluids, a spectrophotometric method based on the molybdenum (Mo) blue reaction was employed as previously described (Prieto *et al.* 1999). The assay is based on the reduction of Mo(VI) to Mo(V) by the sample analyte and the subsequent formation of a blue-colored phosphate/Mo(V) complex at acidic pH. Larval bodies of control (w^{1118}/Y) and $Gclc^{46}/Y$ second-instar larvae (48 hr AEL) were severed on parafilm, followed by dropping 20 μl distilled water on 40 dissected larvae. Ten microliters of the body-fluid–water mixture was taken and mixed with 100 μl of reagent solution [1.3% ammonium molybdate (Sigma), 0.02% dipotassium hydrogen phosphate (Wako), and 1.4 M sulfuric acid (Nacalai Tesque)]. The samples were incubated in a thermal block at 95° for 90 min. After the samples cooled to room temperature, their absorbance was measured at 695 nm against a blank. As a series (0–100 mg/ml) of solutions of L(+)-ascorbic acid (Nacalai Tesque) were used as the standard, the antioxidant capacity was expressed in ascorbic acid equivalents. Values of antioxidant capacity were also normalized by the amount of protein in larval body fluids, measured by the Bradford protein assay (Bradford 1976) with a Qubit protein assay kit and a Qubit 2.0 fluorometer (Thermo Fisher Scientific).

Oxidative stress treatment

Methyl viologen dichloride hydrate, *i.e.*, paraquat (PQ), was used as an oxidative stress inducer as previously described (Jünger *et al.* 2003; Jumbo-Lucioni *et al.* 2013). PQ medium was composed of 0.8% electrophoresis-grade agarose (Nacalai Tesque), 10% sucrose (Nacalai Tesque), and 20 mM PQ (Sigma) in PBS. PQ was added to the solution after cooling to 40°. Control medium was sucrose–agar without PQ. Thirty

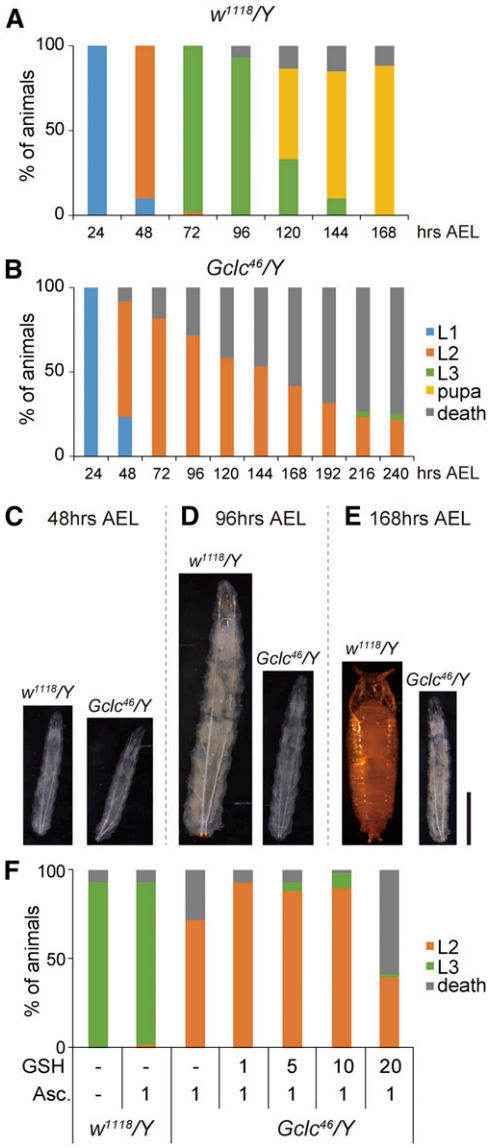

Figure 2 Larval lethality and developmental-arrest phenotype of $Gclc^{46}/Y$ larvae. (A and B) The survival rate and developmental progression of control w^{1118}/Y (A) and $Gclc^{46}/Y$ (B) animals. L1, L2, and L3 indicate first-, second-, and third-instar larvae, respectively. N = 60. (C–E) Comparison of body size and developmental stage between control w^{1118}/Y (left) and $Gclc^{46}/Y$ (right) animals. Typically, control animals were second-instar larvae, third-instar larvae, and pupae at 48 hr (C), 96 hr (D), and 168 hr (E) after egg laying (AEL), respectively. In contrast, $Gclc^{46}/Y$ animals in these photos are all second-instar larvae, collected at the same time points. Bar, 0.5 mm. (F) The larval-arrest phenotype of $Gclc^{46}/Y$ animals was partly rescued by oral administration of glutathione (GSH) from food. The survival rate and developmental progression of w^{1118}/Y and $Gclc^{46}/Y$ animals at 96 hr AEL, fed standard food supplemented with vehicle ethanol (−) with or without GSH and ascorbic acid (Asc.) just after hatching. GSH concentration in food ranged 0–20 mg/ml. Asc. concentration was 1 mg/ml. N = 60.

second-instar larvae at 48 hr AEL were each collected and transferred to vials containing 5 ml of PQ medium or control medium. Twelve hours after the transfer, the number of surviving and dead larvae (60 hr AEL) was counted ($N = 120$ for each condition).

Quantitative reverse transcription (RT)-PCR

RNA isolation, cDNA synthesis, and quantitative RT-PCR reactions were performed as previously described (Enya *et al.* 2014). Total RNA from several tissues of third-instar larvae and adults of the w^{1118} strain were used. To extract total RNA from the ring glands in the third-instar larval stage, we collected the second-instar larvae at 60 hr AEL and let them molt to the third-instar stage in 6 hr. These larvae were dissected at various hours after L2–L3 molting (hr A3L). The primers for quantifying *Gclc* were 5′-CTCACGCGTAA CATTCGCAAGC-3′ and 5′-CAAGCAACAGCAGCCCATGC-3′. Primers amplifying *neverland* (*nvd*), *nobo*, and *rp49* were previously described (Foley *et al.* 1993; Yoshiyama *et al.* 2006; Enya *et al.* 2014). Expression levels were normalized to *rp49* in the same sample. Serial dilutions of a plasmid containing the ORF of each gene were used as a standard.

Transgenic rescue experiment

The GAL4/upstream activating sequence (UAS) system (Brand and Perrimon 1993) was used to overexpress genes in *D. melanogaster*. *UAS-Gclc#3* and *UAS-Gclc#6* (Orr *et al.* 2005) were used to overexpress *Gclc* genes under the control of various tissue-specific *GAL4* drivers. These *UAS* lines carry the same pUAST construct, but the constructs in the *#3* and *#6* strains are located on the third and second chromosome, respectively. The following 11 strains were established and used for transgenic rescue experiments: (1) w^{1118}; *UAS-Gclc#6/CyO*; *TM3 Sb//TM6 Tb*, (2) w^{1118}; *Roi/CyO*; *UAS-Gclc#3/TM3 Sb*, (3) w^{1118}; *UAS-Gclc#6/CyO*; *tubP-GAL4/TM3 Sb*, (4) w^{1118}; *UAS-Gclc#6*; *phm-GAL4#22/TM3 Sb*, (5) w^{1118}; *phm-GAL4#22 UAS-Gclc#3/TM3 Sb*, (6) w^{1118}; *arm-GAL4 UAS-Gclc#6/CyO*, (7) w^{1118}; *ppl-GAL4/CyO*; *UAS-Gclc#3/TM3 Sb*, (8) w^{1118}: *elav-GAL4 UAS-GFP/CyO*; *UAS-Gclc#3/TM3 Sb*, (9) w^{1118}; *UAS-Gclc#6*; *byn-GAL4 UAS-RFP/TM3 Sb*, (10) w^{1118}; *p{GawB} NP3084/CyO*; *UAS-Gclc#3/TM3 Sb*, and (11) w^{1118}; *UAS-Gclc#6*; *mef2-GAL4/TM3 Sb*. Parental males of these flies carrying both *GAL4* and *UAS* constructs were crossed with parental *Gclc^{46}/FM7 act-GFP* females. In the next generation, the number of adult offspring males (*Gclc^{46}/Y* with *GAL4* and *UAS*) and females (*Gclc^{46}/+* with *GAL4* and *UAS*) was counted (Table 2).

Germline mosaic clone analysis

The FLP-DFS technique was performed as previously described (Chou and Perrimon 1992). Virgin females of *Gclc^{46} FRT19Aneo/FM7 act-GFP* were crossed with males of *hsFLP ovoD* y^1 w^{1118} sn^3 *FRT19A/C(1)DX*, y^1 w^1 f^1. By the late second/third-instar stages, the progeny were heat-shocked at 37° for 2 hr over the successive 3 days. When adults were eclosed, virgin females of *Gclc^{46} FRT19A/hsFLP ovoD FRT19A* were crossed with males of w^{1118}.

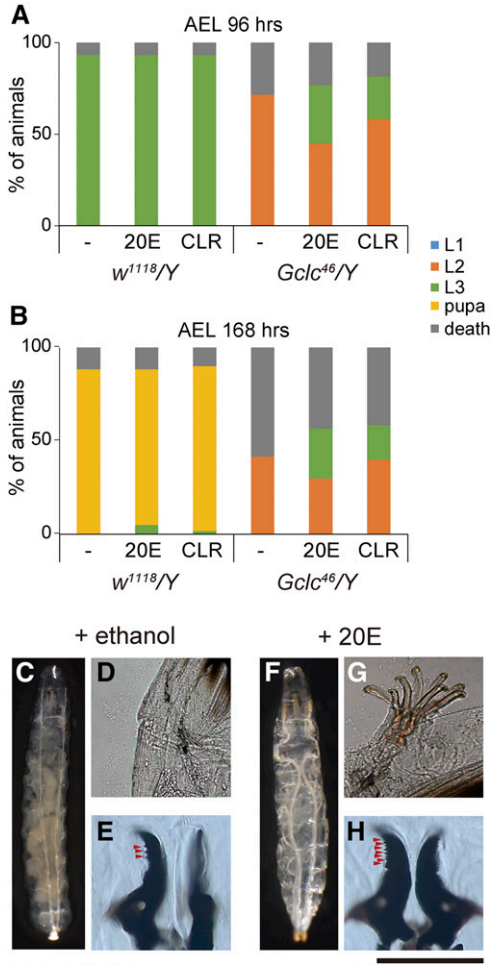

Figure 3 Molting defect of *Gclc^{46}/Y* animals is rescued by feeding 20-hydroxyecdysone (20E) and cholesterol. (A and B) The survival rate and developmental progression of control w^{1118}/*Y* and *Gclc^{46}/Y* animals that were fed standard food supplemented with vehicle ethanol (−), 20E, and cholesterol (CLR). The number of larvae was counted at 96 hr (A) and 168 hr (B) after egg laying (AEL). L1, L2, and L3 indicate first-, second-, and third-instar larvae, respectively. $N = 60$. (C–H) Whole bodies (C and F), anterior tracheal pits (D and G), and dissected mouth hooks (E and H) of *Gclc^{46}/Y* larvae at 96 hr AEL. The animals were reared on standard food supplemented with control ethanol (C–E) and 20E (F–H). *Gclc^{46}/Y* larvae raised on a control diet died in the second-instar larval stage, exhibiting singular insertions of anterior tracheal pits (D) and 2–5 teeth on mouth hooks ((E); red arrowheads). In contrast, 20E-fed *Gclc^{46}/Y* larvae molted in the third-instar larval stage as judged by the branched morphology of the anterior tracheal pits (G) and numerous small teeth on the mouth hook ((H); red arrowheads), typical features of third-instar larvae. Bars, 1 mm for (C and F), 148 μm for (D and G), and 125 μm for (E and H).

The progeny of homozygous *Gclc^{46}* germline clones completed embryogenesis and larval development.

Data availability

All strains and materials are available upon request. Supplemental Material, File S1 contains detailed descriptions of animal count data represented in Figure 2, Figure 3, Figure 4, Figure 6, and Figure 7.

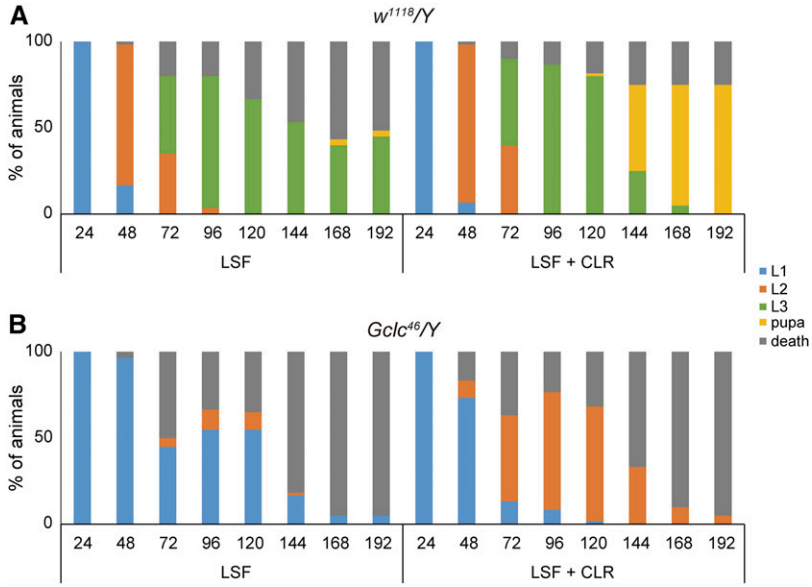

Figure 4 Molting defect of *Gclc*^{46}*/Y* animals is enhanced by low-sterol food (LSF). The survival rate and developmental progression of control *w*^{1118}*/Y* (A) and *Gclc*^{46}*/Y* (B) animals on LSF and cholesterol-supplemented LSF (LSF + CLR). L1, L2, and L3 indicate first-, second-, and third-instar larvae, respectively. *N* = 60.

Results

Generation of complete Gclc loss-of-function allele in D. melanogaster

We first generated a complete *Gclc* loss-of-function allele using CRISPR/Cas9-dependent genome-editing technology (Kondo 2014). We succeeded in isolating the allele called *Gclc*^{46}, which has a 46-bp deletion 185 bp downstream of the start codon (Figure 1, B and C). The predicted protein encoded by the *Gclc*^{46} allele lacks a large portion of the C-terminus, which contains amino acid residues critical for GCL's enzymatic activity (Abbott *et al.* 2002; Hamilton *et al.* 2003) (Figure 1D).

We next examined whether *Gclc*^{46} mutant animals exhibited GSH deficiency *in vivo*. We utilized *Gclc*^{46}*/Y* hemizygous males for subsequent analyses, as *Gclc* is located on the X chromosome, making it technically difficult to obtain homozygous *Gclc* mutant females by conventional genetic crossing. Mass-spectrometric analysis revealed that hemolymph GSH in *Gclc*^{46}*/Y* larvae was undetectable, indicating significant reduction compared to control larvae (Figure 1E). These results suggest that *Gclc*^{46} is a complete loss-of-function allele and causes drastic GSH deficiency.

Gclc mutant animals exhibit developmental arrest at the second-instar larval stage

Similar to a phenotype of mutants lacking a large fragment of the 5′ untranslated region of *Gclc* (Luchak *et al.* 2007), *Gclc*^{46}*/Y* hemizygous mutant animals were lethal. We examined the lethal phase for *Gclc*^{46}*/Y* animals in more detail. *Gclc*^{46}*/Y* animals completed embryogenesis, hatched normally, and showed no apparent morphological defects in the first- and second-instar larval stages (Figure 2, A–C). However, most *Gclc*^{46}*/Y* animals showed arrested development in the second-instar larval stage (Figure 2, B and D), and never became third-instar larvae, pupae, or adults (Figure 2, B and E). As described later, we confirmed that the lethality of *Gclc*^{46}*/Y* animals was rescued by transgenic expression of *Gclc*, suggesting that the observed lethality did not result from off-target mutations by CRISPR/Cas9.

Oral administration of GSH to partly rescue second-instar larval-arrest phenotype of Gclc mutants

To clarify that the second-instar larval-arrest phenotype of *Gclc*^{46}*/Y* was caused by loss of GSH, we conducted a feeding rescue experiment to examine whether oral administration of GSH rescued the phenotype. Feeding standard food mixed with GSH did not rescue the second-instar larval-arrest phenotype of *Gclc*^{46}*/Y* animals (data not shown). Since GSH is easily oxidized in the environment and converted into GSSG, which loses the antioxidant capacity (Sies 1999; Aquilano *et al.* 2014), we speculated that a large portion of GSH mixed with food might convert to the inactive GSSG. Thus, we next conducted feeding rescue experiments using standard food containing not only GSH but also ascorbic acid, a well-known reducing agent, to prevent the conversion of GSH to GSSG. Oral administration of ascorbic acid alone did not rescue the second-instar larval-arrest phenotype of *Gclc*^{46}*/Y* animals (Figure 2E). In contrast, we found that a small but significant number of *Gclc*^{46}*/Y* animals developed to third-instar larvae on standard food supplemented with both 5–20 mg/ml GSH and 1 mg/ml ascorbic acid (Figure 2E). These results suggest that, at least in part, the phenotype observed upon *Gclc* loss-of-function is due to loss of GSH *in vivo*.

The second-instar larval-arrest phenotype of the Gclc mutant is due to loss of ecdysteroids

The larval-arrest phenotype of the *Gclc*^{46}*/Y* mutant phenotype was reminiscent of that of partial loss-of-function animals of several ecdysteroidogenic genes, such as *shroud* RNAi and *nobo* RNAi animals (Niwa *et al.* 2010; Enya *et al.* 2014). Thus, we next examined whether the larval-arrest phenotype

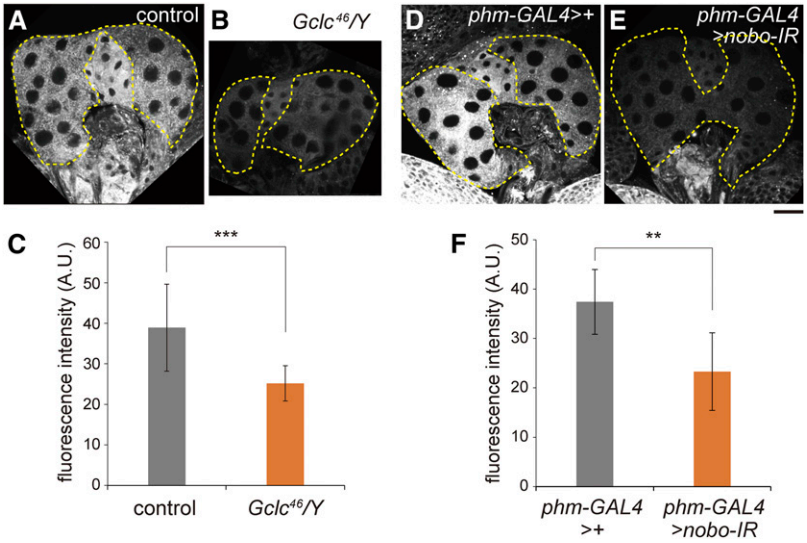

Figure 5 Nile Red staining signals are reduced in the prothoracic gland of *Gclc*^{46}*/Y* and *nobo* RNAi animals. (A, B, D, and E) Fluorescence images of the prothoracic gland (PG) from control *w*^{1118}*/Y* (A), *Gclc*^{46}*/Y* (B), *w*^{1118}; *UAS-dicer2/+*; *phm-GAL4#22/+* (D), and *w*^{1118}; *UAS-dicer2/+*; *phm-GAL4#22/UAS-nobo-IR*(*#40316GD*) (E) stained with Nile Red. All animals were in the second-instar larval stage. Areas of the PGs are outlined by dotted lines. Bar, 20 μm. (C and F) Quantification of Nile Red staining signals in the PG area by ImageJ software. (C) $N = 10$. (F) $N = 11$. ** $P < 0.01$ and *** $P < 0.001$ by Student's *t*-test. It should be noted that, even though *nobo* function was inhibited only in the PG, Nile Red fluorescence was reduced not only in the PG, but also in the corpora allata and the corpora cardiaca for unknown reasons.

of *Gclc*^{46}*/Y* animals was due to the loss of ecdysteroids. We first examined ecdysteroid titer in second-instar larvae (50 hr AEL) of control (*w*^{1118}*/Y*) and *Gclc*^{46}*/Y* animals by mass-spectrometric analysis. In control larvae, we detected 9.87 ± 2.82 pg of 20E equivalent/mg of wet weight (mean ± SEM, $N = 5$). In contrast, among five independent samples of *Gclc*^{46}*/Y* larvae, ecdysteroid titer in three samples was below the quantifiable limit under the same experimental conditions (See *Materials and Methods*). The titer in the two other samples also showed a significantly lower amount (6.22 ± 1.62 pg of 20E/mg of wet weight).

We also found that a considerable number of *Gclc*^{46}*/Y* animals were able to grow to the third-instar larval stage when they were fed standard food containing 20E just after hatching (Figure 3). It should be noted that oral administration of 20E did not allow *Gclc*^{46}*/Y* animals to increase their body size during the third-instar larval stage, to become pupae, or reach later stages (Figure 3, A and B). These results suggest that *Gclc* loss-of-function impairs ecdysteroid biosynthesis during larval development, with *Gclc* appearing to have pivotal roles other than ecdysteroid biosynthesis.

Gclc is involved in the regulation of the behavior of cholesterol

Considering that the Halloween gene *nobo* encodes a GST, we wondered whether a relationship exists between *Gclc* and *nobo* for larval development. To address this question, we first performed a feeding experiment with cholesterol, as the *nobo* loss-of-function phenotype in *D. melanogaster* is well rescued by oral administration of cholesterol (Chanut-Delalande *et al.* 2014; Enya *et al.* 2014). When *Gclc*^{46}*/Y* animals were fed standard food supplemented with cholesterol just after hatching, 18% of the animals developed to third-instar larvae, while failing to increase their body size during the third-instar larval stage and grow into pupae or adults (Figure 3, A and B). The rescue ability of cholesterol for *Gclc*^{46}*/Y* animals was similar to that of 20E as described above (Figure 3, A and B).

Conversely, we took an approach using LSF (see *Materials and Methods*). Under our experimental conditions, most control animals fed LSF arrested in the second- or third-instar larval stage, and never grew to pupae or adults (Figure 4A). This phenotype was restored by cholesterol-supplemented LSF, indicating that the larval-arrest phenotype with LSF is due to sterol depletion. We found that the larval-arrest phenotype of *Gclc*^{46}*/Y* animals was significantly enhanced in LSF as compared to that in cholesterol-supplemented LSF (Figure 4B). Most *Gclc*^{46}*/Y* animals fed LSF arrested in the first-instar larval stage, demonstrating that the larval-arrest phenotype of *Gclc* mutants is sensitively affected by the amount of cholesterol in food.

We next examined whether cellular accumulation of neutral lipids, including cholesterol, was affected in PG cells of *Gclc*^{46}*/Y* and *nobo* RNAi second-instar larvae by Nile Red staining (Figure 5). In the control larvae, neutral lipids were highly accumulated in the ring gland, which contains the PG cells, the corpora allata, and the corpora cardiaca. In contrast, the signals were significantly reduced in the ring gland of the *Gclc*^{46}*/Y* mutant larvae (Figure 5, B and C). We also observed significant reduction of Nile Red signals in the second-instar larvae of *nobo* RNAi animals

Table 1 The larval arrest phenotype of *nobo* RNAi animals is enhanced by *Gclc*^{46} mutation

phm-GAL4#22>dicer2, nobo-IR	Control	*Gclc*^{46}
L1	16	33
L2	41	5
Total	57	38

We combined *Gclc*^{46} mutation with prothoracic gland (PG)-specific *nobo* RNA interference (RNAi), and scored developmental stages of larvae 70–94 hr after egg laying (AEL). *Gclc*^{46} mutant genotype: *Gclc*^{46}*/Y*; *UAS-dicer2/UAS-nobo-IR*(*#101884KK*); *phm-GAL4#22/+*. Control genotype: *FM7/Y*; *UAS-dicer2/UAS-nobo-IR*(*#101884KK*); *phm-GAL4#22/+*. After counting the number of the first- and second-instar larvae, genomic DNA from each individual was extracted, and then the genotype of each individual was determined by genomic PCR. The PCR products of *Gclc*^{WT} and *Gclc*^{46} alleles are separable as shown in Figure 1C. In this analysis, we could exclude *Gclc*^{46} heterozygous females (genotype: *Gclc*^{46}*/FM7*; *UAS-dicer2/UAS-nobo-IR*; *phm-GAL4#22/+*) by genomic PCR, as *Gclc*^{46}*/FM7* females gave rise to multiple PCR bands (236 and 190 bp).

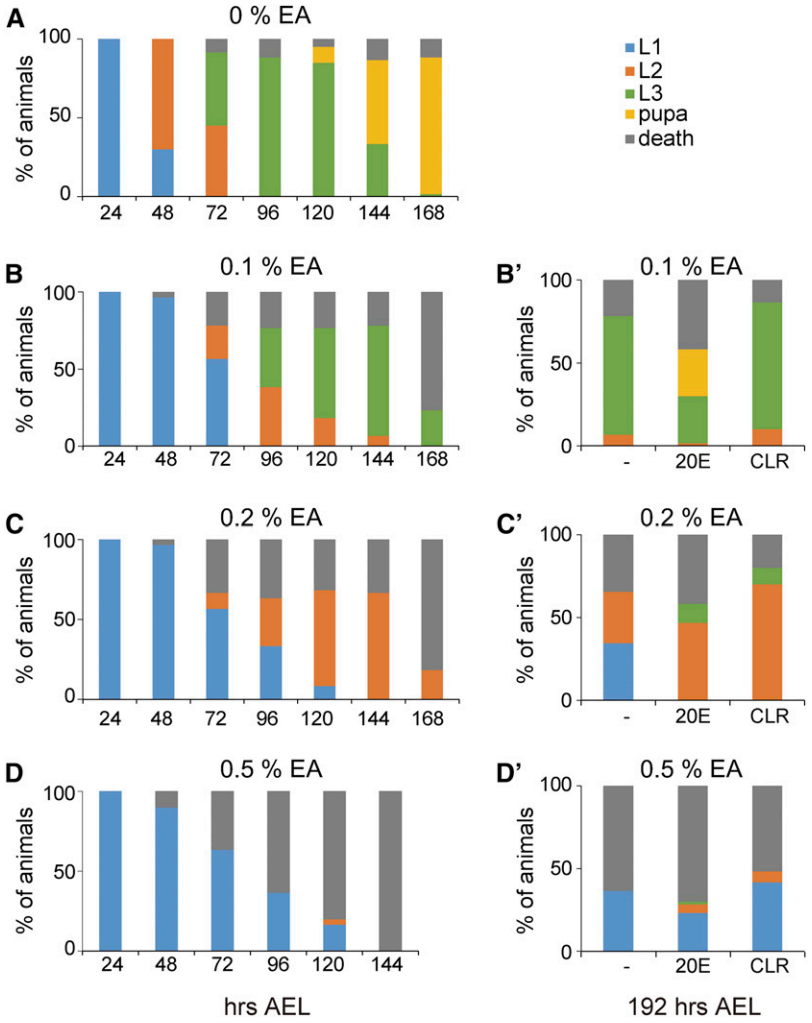

Figure 6 Larval-arrest phenotype induced by ethacrynic acid (EA) is rescued by feeding 20-hydroxyecdysone (20E) and cholesterol (CLR). (A–D) The survival rate and developmental progression of wild-type (w^{1118}) animals that were fed standard food supplemented with vehicle ethanol 0%, (A), 0.1% (B), 0.2% (C), and 0.5% (D) EA. (B'–D') The survival rate at 192 hr after egg laying (AEL) was examined when vehicle ethanol (−), 20E, and CLR were added with 0.1% (B'), 0.2% (C'), and 0.5% (D') EA to standard food. L1, L2, and L3 indicate first-, second-, and third-instar larvae, respectively. $N = 60$.

(Figure 5, D–F). Based on the reminiscent phenotype between $Gclc^{46}/Y$ and *nobo* RNAi animals (Figure 5, B and E), these results suggest that Gclc is involved in cholesterol transport and/or metabolism, as is the case with Nobo.

Gclc genetically interacts with nobo for larval development

To gain insights into a genetic interaction between *Gclc* and *nobo*, we examined whether the developmental arrest phenotype by *nobo* RNAi was enhanced by *Gclc* mutation. For this purpose, we combined $Gclc^{46}$ mutation with PG-specific *nobo* RNAi. More than 70% of control larvae (*FM7/Y*; *phm* > *dicer2*, *nobo-IR*) were in the second-instar larval stage 70–94 hr AEL (Table 1). In contrast, only 13% of the double mutants ($Gclc^{46}/Y$; *phm* > *dicer2*, *nobo-IR*) became the second-instar larvae, and the majority of them remained in the first-instar larval stage (Table 1). These results suggest that *Gclc* function is coupled with Nobo for larval development.

GST inhibitor-treated larvae phenocopy Gclc mutant animals

To further support our hypothesis that GSH is primarily essential for larval developmental progression, dependent on GST activity, we conducted a feeding experiment of wild-type animals with the general GST inhibitor ethacrynic acid(EA) (Awasthi *et al.* 1993). We previously demonstrated that EA inhibits Nobo enzymatic activity using an artificial substrate *in vitro* (Fujikawa *et al.* 2015). When the wild-type larvae were raised on EA-containing food, they resulted in a developmental-arrest phenotype in a dose-dependent manner (Figure 6, A–D). Moreover, the EA-induced larval-arrest phenotype was rescued by coadministration of 20E or cholesterol (Figure 6, B'–D'). Thus, EA-treated animals phenocopied *Gclc* mutant animals in terms of the larval-arrest phenotype. These results provide us with another line of evidence showing that *Gclc* is required for larval development through the function of GST, possibly via Nobo.

Gclc mutant animals exhibit significant reduction in antioxidant capacity

One of the most crucial roles of GSH is the maintenance of redox homeostasis, providing reducing equivalents for the elimination of reactive oxygen species. We therefore investigated whether *Gclc* mutant animals displayed any defects in the antioxidant system in *D. melanogaster* larvae.

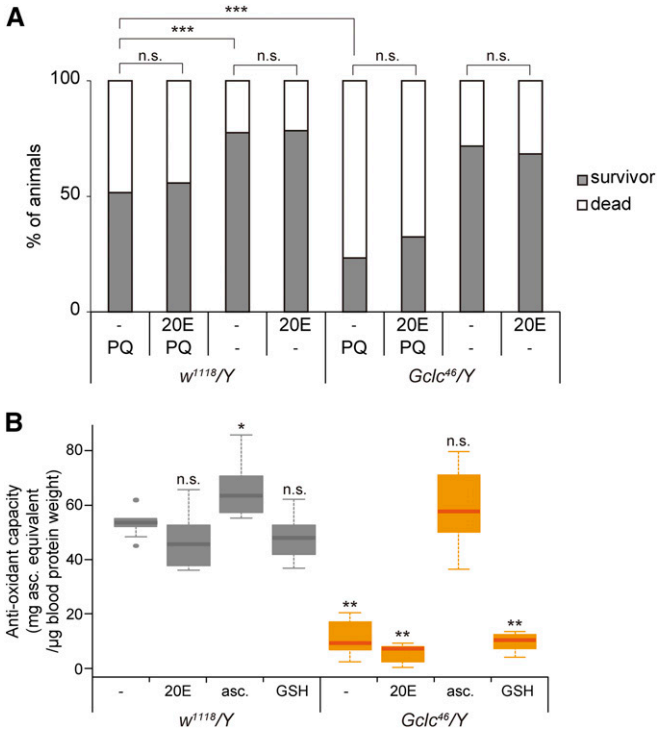

Figure 7 Oxidative stress response and antioxidant-capacity phenotypes of *Gclc*^{46}*/Y* are not rescued by 20-hydroxyecdysone (20E) administration. (A) The survival rate and developmental progression of control *w*^{1118}*/Y* and *Gclc*^{46}*/Y* animals that were fed sucrose-agar medium containing paraquat (PQ) and/or 20E. Second-instar larvae at 48 hr after egg laying (AEL) were transferred to the medium, then fed media for 12 hr. *** $P < 0.001$ chi-square test with Bonferroni correction. n.s., not significant. (B) Antioxidant capacity of body fluids isolated from control *w*^{1118}*/Y* and *Gclc*^{46}*/Y* second-instar larvae (60 hr AEL) that were fed standard food supplemented with vehicle ethanol (−), 20E, ascorbic acid (asc.), and glutathione (GSH). * $P < 0.05$ and ** $P < 0.01$ by Dunnett's test.

We first examined whether the sensitivity to oxidative stress was changed between control and *Gclc*^{46}*/Y* larvae, as *Gclc* RNAi adult flies are less resistant to oxidative stress (Luchak *et al.* 2007). The second-instar larvae of control and *Gclc*^{46}*/Y* animals were fed a sucrose–agar medium containing the well-known oxidative stress inducer PQ for 12 hr. The medium did not contain rich nutrients and the survival rate of control animals fed the medium without PQ was 78% (Figure 7A). Under these experimental conditions and on PQ medium, a smaller number (52%) of control animals survived. In contrast, much fewer (23%) *Gclc*^{46}*/Y* larvae survived on PQ medium (Figure 7A).

We next examined the antioxidant capacity of *Gclc* mutant animals. We utilized an established spectrophotometric method based on the Mo blue reaction (Prieto *et al.* 1999) to quantitatively determine the capacity of larval body fluids. Consistent with the hypersensitivity to oxidative stress, we found that body fluid from *Gclc*^{46}*/Y* larvae exhibited a significant reduction in antioxidant capacity compared to control animals (Figure 7B). These results suggest that loss of GSH in *Gclc* mutants leads to defective antioxidant capacity.

Importantly, neither antioxidant capacity nor the hypersensitivity-to-oxidative stress phenotype of second-instar *Gclc*^{46}*/Y* larvae was rescued by oral administration of 20E (Figure 7, A and B). In addition, oral administration of ascorbic acid restored antioxidant capacity (Figure 7B) but did not rescue the second-instar larval-arrest phenotype of *Gclc*^{46}*/Y* larvae (Figure 2F). Given that 20E administration rescued the second-instar larval-arrest phenotype of *Gclc*^{46}*/Y* animals, allowing them to grow to the third-instar larval stage, these results suggest that the larval-arrest phenotype of *Gclc* mutant animals does not correlate with the antioxidant-capacity defect. In other words, the primary role of GSH during the early larval stage is to be involved in ecdysteroid biosynthesis, but not maintenance of redox homeostasis.

Rescue of larval-arrest phenotype of Gclc mutant by Gclc transgene

To address the functional specificity of Gclc in the PG, we performed a quantitative RT-PCR experiment to investigate the tissue distribution of the *Gclc* transcript. In the late third-instar larval stage, *Gclc* was highly expressed in the ring gland as compared to other tissues (Figure 8A), consistent with a previous transcriptome study (Ou *et al.* 2016). We also examined a temporal expression pattern of *Gclc* and *nobo* in addition to *neverland* (*nvd*), encoding the cholesterol 7,8-dehydrogenase for ecdysteroid biosynthesis (Yoshiyama *et al.* 2006; Yoshiyama-Yanagawa *et al.* 2011). In the ring glands of the third-instar larvae, the temporal fluctuation of *Gclc* transcript was well correlated with those of *nobo* and *nvd* transcripts (Figure 8B), suggesting that the expression of *Gclc* is coupled to ecdysteroid biosynthesis in the PG. On

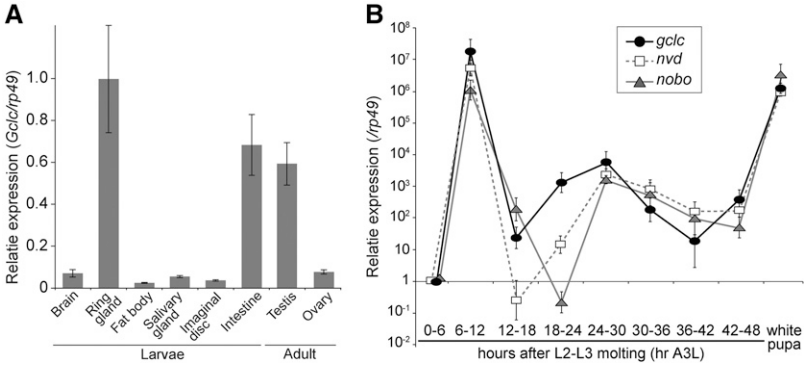

Figure 8 The spatiotemporal expression profile of *Gclc* in the third-instar larvae. (A) *Gclc* mRNA amounts were quantified by quantitative RT-PCR. Total RNA samples were prepared from several tissues in wandering third-instar larvae and adult flies. The normalized *Gclc* mRNA level in the ring gland is set as 1. (B) Total RNA samples were prepared from the ring glands of third-instar larvae. The relative expression levels of *Gclc*, *nvd*, and *nobo* were normalized to the levels of 0–6 hr after L2–L3 molting (hr A3L). Each error bar represents the SEM from at least three independent samples.

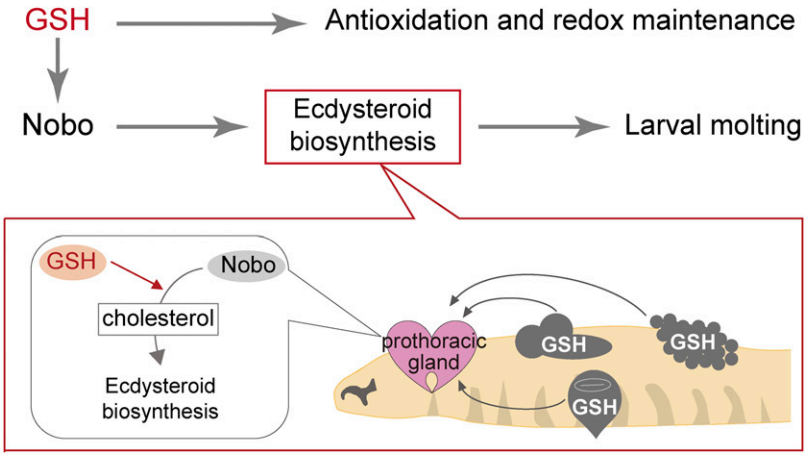

Figure 9 Model of the systemic action of glutathione (GSH) in controlling larval development.

the other hand, weaker, yet considerable, expression was observed in many larval tissues other than the PG (Figure 8A). This is in a sharp contrast with *nobo* and *nvd*, which are predominantly expressed in the PG during larval development (Yoshiyama *et al.* 2006; Enya *et al.* 2014).

To test if *Gclc* is cell autonomously required in the PG, we induced PG-specific RNAi against *Gclc* by using *phm-GAL4#22* and two independent transgenic *UAS*-RNAi lines (see *Materials and Methods*). Unexpectedly, the PG-specific *Gclc* RNAi larvae exhibited no obvious developmental arrest phenotypes and normally grew up to adulthood (Table S1). This result implies the possibility that Gclc function in tissues other than the PG might affect ecdysteroid biosynthesis.

To address this possibility, we conducted tissue-specific overexpression experiments. The lethality of $Gclc^{46}/Y$ animals was rescued by expression of the *UAS-Gclc* transgene driven by the ubiquitous *tubP-GAL4* driver (Table 2). In addition, the lethality of $Gclc^{46}/Y$ animals was rescued by expression of *Gclc* in the PG cells by the *phm-GAL4* driver, consistent with the idea that GSH plays an essential role in the PG. Unexpectedly, the $Gclc^{46}/Y$ lethal phenotype was also rescued to some degree by several *GAL4* drivers that were active in restricted types of tissues or cells other than the PG, including the fat body (*ppl-GAL4*), the nervous system (*elav-GAL4*), the hindgut (*byn-GAL4*), and the wider gut area (*NP3084*), but not the muscle (*Dmef2-Gal4*) (Table 2). These results raise the interesting possibility that GSH biosynthesized in peripheral tissues other than the PG might systemically circulate and affect ecdysteroid biosynthesis in the PG.

Discussion

In this study, we report the effect of GSH deficiency employing genetic, developmental, and physiological approaches, using complete *Gclc* loss-of-function mutant animals of *D. melanogaster*. It is widely accepted that GSH serves as not only the substrate of GSTs but also the most abundant intracellular nonprotein thiol in most organisms. Indeed, a number of pioneering studies using adult *D. melanogaster* have supported the antioxidant role of GSH in maintaining redox homeostasis (Orr *et al.* 2005; Luchak *et al.* 2007; Beaver *et al.* 2012; Radyuk *et al.* 2012; Klichko *et al.* 2015; Mercer *et al.* 2016; Moskalev *et al.* 2016). In this sense, the unexpected finding in this study is that the second-instar larval-arrest phenotype of *Gclc* mutant animals is not due to defective antioxidant function, but rather due to an impairment of ecdysteroid biosynthesis. Given that the ecdysteroid biosynthesis pathway requires a specialized GST, namely Nobo, we propose our hypothesis that GSH is primarily important for ecdysteroid biosynthesis through the regulation of the enzymatic activity of Nobo during early larval development (Figure 9).

However, it must be noted that GSH loss *in vivo* may also result in pleiotropic effects in the PG, as GSH is involved in many biological processes such as antioxidant function and xenobiotics. We cannot completely rule out the possibility that ecdysteroid biosynthesis is indirectly affected, independently from Nobo function. In future studies, it would be worth examining whether a mutated Nobo protein that selectively abolishes GSH binding is dysfunctional for ecdysteroid biosynthesis or not.

Table 2 Viability of $Gclc^{46}/Y$ animals expressing *Gclc*

GAL4 drivers[a]	Tissues/cells in which *GAL4* is active	Number of adults
*-*1*	No GAL4	0 (129)
*-*2*	No GAL4	0 (101)
*tubP-GAL4*1*	Ubiquitous	35 (34)
*phm-GAL4#22*1*	PG	21 (104)
*phm-GAL4#22*2*	PG	56 (124)
*arm-GAL4*2*	Epithelial cells	94 (95)
*ppl-GAL4*2*	Fat body	48 (95)
*elav-GAL4*2*	Nerve system	61 (74)
*byn-GAL4*1*	Hindgut	32 (68)
*NP3084*2*	Gut	54 (55)
*Dmef2-GAL4*1*	Muscle	1 (165)

The number of viable $Gclc^{46}/Y$ adults was scored. Transgenes were driven by several *GAL4* drivers. Details of this experiment are described in the *Materials and Methods*. Values in parentheses indicate the number of viable control $Gclc^{46}/+$ heterozygous females from the parental strains in the same experimental batches. PG, prothoracic gland.

[a] *1, *UAS-Gclc#6* was used, *2, *UAS-Gclc#3* was used.

We must also take into consideration that GSH plays crucial roles in physiological processes other than ecdysteroid biosynthesis after the third-instar larval stage. This consideration is based on our observation that *Gclc*^{46}/*Y* animals on a 20E-supplemented diet never grow into later third-instar larvae or pupae. One possibility is that GSH serves as a substrate for not only Nobo, but also other nonecdysteroidogenic GSTs in developing third-instar larvae and pupae. The *D. melanogaster* genome possesses at least 36 independent cytosolic GSTs (Wai *et al.* 2007). Previous studies have demonstrated that a number of cytosolic GST genes are expressed in cells other than PG cells, such as neurons and midgut cells, of third-instar larvae (Li *et al.* 2008; Deng and Kerppola 2013, 2014; Harrop *et al.* 2014). Some of these genes are responsible for the xenobiotic response. Related to this point, a recent important finding is that the CncC-dKeap1 pathway, a major upstream regulator of xenobiotic detoxification, is essential for the larva-to-pupa transition and has significant effects on transcription of the *GSTd1* and *GSTe1* xenobiotic response genes (Deng and Kerppola 2013, 2014). Thus, GCLc-dependent GSH biosynthesis might play more versatile roles in later development as compared to earlier larval development.

Our study shows that *Gclc*^{46}/*Y* animals can complete embryogenesis and first-instar larval development. In contrast, complete *nobo* loss-of-function animals exhibit embryonic lethality with typical Halloween mutant phenotypes (Chanut-Delalande *et al.* 2014; Enya *et al.* 2014), implying that GSH is necessary for embryonic development. To address if GSH is maternally loaded into eggs, we generated a *Gclc* germline clone, but observed no obvious phenotype of their offspring (data not shown). This result implies that maternal GSH is not supplied from germline, but instead from somatic follicle cells. Alternatively, GSH could be loaded maternally from food; in the yeast *Saccharomyces cerevisiae*, which is contained in the standard food for rearing *D. melanogaster*, GSH is present in high concentrations of up to 10 mM (Penninckx 2002).

Another important finding in this study is that GSH might systemically circulate throughout the larval body to be eventually taken up by PG cells (Figure 9). To incorporate extracellular GSH into PG cells, GSH transporters must be present in the hemolymph. In *S. cerevisiae* and the plant *Arabidopsis thaliana*, Hgt1p and AtOPT4 are identified as high-affinity GSH transporters (Bourbouloux *et al.* 2000; Zhang *et al.* 2016), while their orthologs have not been found in animal genomes. In mammals, two organic-anion transporters, OAT1 and OAT3, are potential candidates that may be responsible for extracellular GSH uptake, whereas these transporters seem not to be specific for GSH and their *in vivo* function has not been evaluated (Bachhawat *et al.* 2013). Further studies are required for the identification and characterization of GSH transporters underlying the systemic action of GSH in animals.

It has been reported that GSH amounts and redox status fluctuate in a temporal and developmental stage-specific manner during zebrafish early embryogenesis (Timme-Laragy *et al.* 2013). Moreover, *Gclc* homozygous knockout mice are embryonic lethal and die before gestational day 13 (Dalton *et al.* 2000). However, a functional role of GCLc and GSH during embryogenesis is still largely unclear, as embryonic phenotypes of *Gclc* mutants in either zebrafish or mice have not been extensively investigated. It would be intriguing to examine whether GSH-dependent steroid hormone biosynthesis is also involved in early developmental processes in vertebrates.

Acknowledgments

We thank Reiko Kise for technical support. We are also grateful to Tobias P. Dick, Ryutaro Murakami, Michael B. O'Connor, Eric N. Olson, William C. Orr, David Ron, Hiroko Sano, Tadashi Uemura, Takeo Usui, Alisa Zyryanova, the Bloomington *Drosophila* Stock Center, Kyoto Stock Center, the Vienna *Drosophila* RNAi Center, and the National Institute of Genetics for stocks and reagents. We thank Akira Ogawa for helpful discussion. S.E. was a recipient of research fellowships for young scientists from the Japan Society for the Promotion of Science (JSPS). This work was supported by JSPS Grants-in-Aid for Scientific Research (KAKENHI) grant numbers 12J01444 to S.E. and 15K14719 to R.N.; Japan Science and Technology Agency (JST) Precursory Research for Embryonic Science and Technology grant number JPMJPR12M1 to R.N.; the Naito Foundation and the Inoue Foundation to Y.S.-N.; and the JST and Japan Agency for Medical Research and Development project for the Development of Systems and Technology for Advanced Measurement and Analysis to T.M.

Literature Cited

Abbott, J. J., J. L. Ford, and M. A. Phillips, 2002 Substrate binding determinants of *Trypanosoma brucei* γ-glutamylcysteine synthetase. Biochemistry 41: 2741–2750.

Aquilano, K., S. Baldelli, and M. R. Ciriolo, 2014 Glutathione: new roles in redox signalling for an old antioxidant. Front. Pharmacol. 5: 196.

Awasthi, S., S. K. Srivastava, F. Ahmad, H. Ahmad, and G. A. Ansari, 1993 Interactions of glutathione S-transferase-π with ethacrynic acid and its glutathione conjugate. Biochim. Biophys. Acta 1164: 173–178.

Bachhawat, A. K., A. Thakur, J. Kaur, and M. Zulkifli, 2013 Glutathione transporters. Biochim. Biophys. Acta, Gen. Subj. 1830: 3154–3164.

Beaver, L. M., V. I. Klichko, E. S. Chow, J. Kotwica-Rolinska, M. Williamson *et al.*, 2012 Circadian regulation of glutathione levels and biosynthesis in *Drosophila melanogaster*. PLoS One 7: e50454.

Bourbouloux, A., P. Shahi, A. Chakladar, S. Delrot, and A. K. Bachhawat, 2000 Hgt1p, a high affinity glutathione transporter from the yeast *Saccharomyces cerevisiae*. J. Biol. Chem. 275: 13259–13265.

Bradford, M. M., 1976 A rapid and sensitive method for the quantitation of microgram quantities of protein utilizing the principle of protein-dye binding. Anal. Biochem. 72: 248–254.

Brand, A. H., and N. Perrimon, 1993 Targeted gene expression as a means of altering cell fates and generating dominant phenotypes. Development 118: 401–415.

Carvalho, M., D. Schwudke, J. L. Sampaio, W. Palm, I. Riezman *et al.*, 2010 Survival strategies of a sterol auxotroph. Development 137: 3675–3685.

Chanut-Delalande, H., Y. Hashimoto, A. Pelissier-Monier, R. Spokony, A. Dib *et al.*, 2014 Pri peptides are mediators of ecdysone for the temporal control of development. Nat. Cell Biol. 16: 1035–1044.

Chávez, V. M., G. Marqués, J. P. Delbecque, K. Kobayashi, M. Hollingsworth *et al.*, 2000 The *Drosophila disembodied* gene controls late embryonic morphogenesis and codes for a cytochrome P450 enzyme that regulates embryonic ecdysone levels. Development 127: 4115–4126.

Chou, T. B., and N. Perrimon, 1992 Use of a yeast site-specific recombinase to produce female germline chimeras in Drosophila. Genetics 131: 643–653.

Colombani, J., S. Raisin, S. Pantalacci, T. Radimerski, J. Montagne *et al.*, 2003 A nutrient sensor mechanism controls *Drosophila* growth. Cell 114: 739–749.

Dalton, T. P., M. Z. Dieter, Y. Yang, H. G. Shertzer, and D. W. Nebert, 2000 Knockout of the mouse glutamate cysteine ligase catalytic subunit (Gclc) gene: embryonic lethal when homozygous, and proposed model for moderate glutathione deficiency when heterozygous. Biochem. Biophys. Res. Commun. 279: 324–329.

Deng, H., and T. K. Kerppola, 2013 Regulation of *Drosophila* metamorphosis by xenobiotic response regulators. PLoS Genet. 9: e1003263.

Deng, H., and T. K. Kerppola, 2014 Visualization of the *Drosophila* dKeap1-CncC interaction on chromatin illumines cooperative, xenobiotic-specific gene activation. Development 141: 3277–3288.

Enya, S., T. Ameku, F. Igarashi, M. Iga, H. Kataoka *et al.*, 2014 A Halloween gene *noppera-bo* encodes a glutathione *S*-transferase essential for ecdysteroid biosynthesis via regulating the behaviour of cholesterol in *Drosophila*. Sci. Rep. 4: 6586.

Enya, S., T. Daimon, F. Igarashi, H. Kataoka, M. Uchibori *et al.*, 2015 The silkworm glutathione *S*-transferase gene *noppera-bo* is required for ecdysteroid biosynthesis and larval development. Insect Biochem. Mol. Biol. 61: 1–7.

Fedulova, N., F. Raffalli-Mathieu, and B. Mannervik, 2010 Porcine glutathione transferase Alpha 2-2 is a human GST A3-3 analogue that catalyses steroid double-bond isomerization. Biochem. J. 431: 159–167.

Finn, R. D., P. Coggill, R. Y. Eberhardt, S. R. Eddy, J. Mistry *et al.*, 2016 The Pfam protein families database: towards a more sustainable future. Nucleic Acids Res. 44: D279–D285.

Foley, K. P., M. W. Leonard, and J. D. Engel, 1993 Quantitation of RNA using the polymerase chain reaction. Trends Genet. 9: 380–385.

Fraser, J. A., R. D. C. Saunders, and L. I. McLellan, 2002 *Drosophila melanogaster* glutamate-cysteine ligase activity is regulated by a modifier subunit with a mechanism of action similar to that of the mammalian form. J. Biol. Chem. 277: 1158–1165.

Fraser, J. A., P. Kansagra, C. Kotecki, R. D. C. Saunders, and L. I. McLellan, 2003 The modifier subunit of *Drosophila* glutamate-cysteine ligase regulates catalytic activity by covalent and noncovalent interactions and influences glutathione homeostasis *in vivo*. J. Biol. Chem. 278: 46369–46377.

Fujii, T., S. Matsuda, M. L. Tejedor, T. Esaki, I. Sakane *et al.*, 2015 Direct metabolomics for plant cells by live single-cell mass spectrometry. Nat. Protoc. 10: 1445–1456.

Fujikawa, Y., F. Morisaki, A. Ogura, K. Morohashi, S. Enya *et al.*, 2015 A practical fluorogenic substrate for high-throughput screening of glutathione S-transferase inhibitors. Chem. Commun. (Camb.) 14: 1–4.

Gilbert, L. I., 2004 Halloween genes encode P450 enzymes that mediate steroid hormone biosynthesis in *Drosophila melanogaster*. Mol. Cell. Endocrinol. 215: 1–10.

Griffith, O. W., and R. T. Mulcahy, 1999 The enzymes of glutathione synthesis: γ-glutamylcysteine synthetase. Adv. Enzymol. Relat. Areas Mol. Biol. 73: 209–267.

Hamilton, D., J. H. Wu, M. Alaoui-Jamali, and G. Batist, 2003 A novel missense mutation in the γ-glutamylcysteine synthetase catalytic subunit gene causes both decreased enzymatic activity and glutathione production. Blood 102: 725–730.

Harrop, T. W. R., S. L. Pearce, P. J. Daborn, and P. Batterham, 2014 Whole-genome expression analysis in the third instar larval midgut of *Drosophila melanogaster*. G3 (Bethesda) 4: 2197–2205.

Hikiba, J., M. H. Ogihara, M. Iga, K. Saito, Y. Fujimoto *et al.*, 2013 Simultaneous quantification of individual intermediate steroids in silkworm ecdysone biosynthesis by liquid chromatography-tandem mass spectrometry with multiple reaction monitoring. J. Chromatogr. B Analyt. Technol. Biomed. Life Sci. 915–916: 52–56.

Igarashi, F., J. Hikiba, M. H. Ogihara, T. Nakaoka, M. Suzuki *et al.*, 2011 A highly specific and sensitive quantification analysis of the sterols in silkworm larvae by high performance liquid chromatography-atmospheric pressure chemical ionization-tandem mass spectrometry. Anal. Biochem. 419: 123–132.

Imura, E., Y. Yoshinari, Y. Shimada-Niwa, and R. Niwa, 2017 Protocols for visualizing steroidogenic organs and their interactive organs with immunostaining in the fruit fly *Drosophila melanogaster*. J. Vis. Exp. 122: e55519.

Iwaki, D. D., and J. A. Lengyel, 2002 A delta-notch signaling border regulated by engrailed/invected repression specifies boundary cells in the *Drosophila* hindgut. Mech. Dev. 114: 71–84.

Jumbo-Lucioni, P. P., M. L. Hopson, D. Hang, Y. Liang, D. P. Jones *et al.*, 2013 Oxidative stress contributes to outcome severity in a *Drosophila melanogaster* model of classic galactosemia. Dis. Model. Mech. 6: 84–94.

Jünger, M. A., F. Rintelen, H. Stocker, J. D. Wasserman, M. Végh *et al.*, 2003 The *Drosophila* Forkhead transcription factor FOXO mediates the reduction in cell number associated with reduced insulin signaling. J. Biol. 2: 20.

Klichko, V. I., E. S. Chow, J. Kotwica-Rolinska, W. C. Orr, J. M. Giebultowicz *et al.*, 2015 Aging alters circadian regulation of redox in *Drosophila*. Front. Genet. 6: 83.

Kondo, S., 2014 New horizons in genome engineering of *Drosophila melanogaster*. Genes Genet. Syst. 89: 3–8.

Kondo, S., and R. Ueda, 2013 Highly improved gene targeting by germline-specific Cas9 expression in *Drosophila*. Genetics 195: 715–721.

Lee, T., and L. Luo, 1999 Mosaic analysis with a repressible cell marker for studies of gene function in neuronal morphogenesis. Neuron 22: 451–461.

Li, H. M., G. Buczkowski, O. Mittapalli, J. Xie, J. Wu *et al.*, 2008 Transcriptomic profiles of *Drosophila melanogaster* third instar larval midgut and responses to oxidative stress. Insect Mol. Biol. 17: 325–339.

Loncle, N., M. Boube, L. Joulia, C. Boschiero, M. Werner *et al.*, 2007 Distinct roles for mediator Cdk8 module subunits in *Drosophila* development. EMBO J. 26: 1045–1054.

Lu, S. C., 2014 Glutathione synthesis. Biochim. Biophys. Acta 1830: 3143–3153.

Luchak, J. M., L. Prabhudesai, R. S. Sohal, S. N. Radyuk, and W. C. Orr, 2007 Modulating longevity in *Drosophila* by over- and underexpression of glutamate-cysteine ligase. Ann. N. Y. Acad. Sci. 1119: 260–273.

Luo, L., Y. J. Liao, L. Y. Jan, and Y. N. Jan, 1994 Distinct morphogenetic functions of similar small GTPases: *Drosophila* Drac1 is involved in axonal outgrowth and myoblast fusion. Genes Dev. 8: 1787–1802.

McBrayer, Z., H. Ono, M. Shimell, J. P. Parvy, R. B. Beckstead *et al.*, 2007 Prothoracicotropic hormone regulates developmental timing and body size in *Drosophila*. Dev. Cell 13: 857–871.

Mercer, S. W., S. La Fontaine, C. G. Warr, and R. Burke, 2016 Reduced glutathione biosynthesis in *Drosophila melanogaster* causes neuronal defects linked to copper deficiency. J. Neurochem. 137: 360–370.

Moskalev, A., M. Shaposhnikov, E. Proshkina, A. Belyi, A. Fedintsev *et al.*, 2016 The influence of pro-longevity gene *Gclc* overexpression on the age-dependent changes in *Drosophila* transcriptome and biological functions. BMC Genomics 17: 1046.

Namiki, T., R. Niwa, T. Sakudoh, K. I. Shirai, H. Takeuchi *et al.*, 2005 Cytochrome P450 CYP307A1/Spook: a regulator for ecdysone synthesis in insects. Biochem. Biophys. Res. Commun. 337: 367–374.

Nehme, N. T., S. Liégeois, B. Kele, P. Giammarinaro, E. Pradel *et al.*, 2007 A model of bacterial intestinal infections in *Drosophila melanogaster*. PLoS Pathog. 3: 1694–1709.

Niwa, R., and Y. S. Niwa, 2014 Enzymes for ecdysteroid biosynthesis: their biological functions in insects and beyond. Biosci. Biotechnol. Biochem. 78: 1283–1292.

Niwa, R., T. Matsuda, T. Yoshiyama, T. Namiki, K. Mita *et al.*, 2004 CYP306A1, a cytochrome P450 enzyme, is essential for ecdysteroid biosynthesis in the prothoracic glands of *Bombyx* and *Drosophila*. J. Biol. Chem. 279: 35942–35949.

Niwa, R., T. Namiki, K. Ito, Y. Shimada-Niwa, M. Kiuchi *et al.*, 2010 *Non-molting glossy/shroud* encodes a short-chain dehydrogenase/reductase that functions in the "Black Box" of the ecdysteroid biosynthesis pathway. Development 137: 1991–1999.

Niwa, Y. S., and R. Niwa, 2014 Neural control of steroid hormone biosynthesis during development in the fruit fly *Drosophila melanogaster*. Genes Genet. Syst. 89: 27–34.

Niwa, Y. S., and R. Niwa, 2016 Transcriptional regulation of insect steroid hormone biosynthesis and its role in controlling timing of molting and metamorphosis. Dev. Growth Differ. 58: 94–105.

Nüsslein-Volhard, C., E. Wieschaus, and H. Kluding, 1984 Mutations affecting the pattern of the larval cuticle in *Drosophila melanogaster*. I. Zygotic loci on the second chromosome. Rouxs Arch. Dev. Biol. 193: 267–282.

Ono, H., K. F. Rewitz, T. Shinoda, K. Itoyama, A. Petryk *et al.*, 2006 *Spook* and *Spookier* code for stage-specific components of the ecdysone biosynthetic pathway in Diptera. Dev. Biol. 298: 555–570.

Orr, W. C., S. N. Radyuk, L. Prabhudesai, D. Toroser, J. J. Benes *et al.*, 2005 Overexpression of glutamate-cysteine ligase extends life span in *Drosophila melanogaster*. J. Biol. Chem. 280: 37331–37338.

Ou, Q., J. Zeng, N. Yamanaka, C. Brakken-Thal, M. B. O'Connor *et al.*, 2016 The insect prothoracic gland as a model for steroid hormone biosynthesis and regulation. Cell Rep. 16: 247–262.

Penninckx, M. J., 2002 An overview on glutathione in *Saccharomyces* versus non-conventional yeasts. FEMS Yeast Res. 2: 295–305.

Petryk, A., J. T. Warren, G. Marqués, M. P. Jarcho, L. I. Gilbert *et al.*, 2003 Shade is the *Drosophila* P450 enzyme that mediates the hydroxylation of ecdysone to the steroid insect molting hormone 20-hydroxyecdysone. Proc. Natl. Acad. Sci. USA 100: 13773–13778.

Prieto, P., M. Pineda, and M. Aguilar, 1999 Spectrophotometric quantitation of antioxidant capacity through the formation of a phosphomolybdenum complex: specific application to the determination of vitamin E. Anal. Biochem. 269: 337–341.

Radyuk, S. N., J. Gambini, C. Borras, E. Serna, V. I. Klichko *et al.*, 2012 Age-dependent changes in the transcription profile of long-lived *Drosophila* over-expressing glutamate cysteine ligase. Mech. Ageing Dev. 133: 401–413.

Raffalli-Mathieu, F., and B. Mannervik, 2005 Human glutathione transferase A3–3 active as steroid double-bond isomerase. Methods Enzymol. 401: 265–278.

Ranganayakulu, G., R. A. Schulz, and E. N. Olson, 1996 Wingless signaling induces *nautilus* expression in the ventral mesoderm of the *Drosophila* embryo. Dev. Biol. 176: 143–148.

Rewitz, K. F., R. Rybczynski, J. T. Warren, and L. I. Gilbert, 2006 The Halloween genes code for cytochrome P450 enzymes mediating synthesis of the insect moulting hormone. Biochem. Soc. Trans. 34: 1256–1260.

Schneider, C. A., W. S. Rasband, and K. W. Eliceiri, 2012 NIH image to ImageJ: 25 years of image analysis. Nat. Methods 9: 671–675.

Sies, H., 1999 Glutathione and its role in cellular functions. Free Radic. Biol. Med. 27: 916–921.

Timme-Laragy, A. R., J. V. Goldstone, B. R. Imhoff, J. J. Stegeman, M. E. Hahn *et al.*, 2013 Glutathione redox dynamics and expression of glutathione-related genes in the developing embryo. Free Radic. Biol. Med. 65: 89–101.

Uryu, O., T. Ameku, and R. Niwa, 2015 Recent progress in understanding the role of ecdysteroids in adult insects: germline development and circadian clock in the fruit fly *Drosophila melanogaster*. Zool. Lett. 1: 32.

Wai, Y. L., L. N. Hooi, C. J. Morton, M. W. Parker, P. Batterham *et al.*, 2007 Molecular evolution of glutathione *S*-transferases in the genus Drosophila. Genetics 177: 1363–1375.

Warren, J. T., A. Petryk, G. Marques, M. Jarcho, J.-P. Parvy *et al.*, 2002 Molecular and biochemical characterization of two P450 enzymes in the ecdysteroidogenic pathway of *Drosophila melanogaster*. Proc. Natl. Acad. Sci. USA 99: 11043–11048.

Warren, J. T., A. Petryk, G. Marqués, J. P. Parvy, T. Shinoda *et al.*, 2004 Phantom encodes the 25-hydroxylase of *Drosophila melanogaster* and *Bombyx mori*: a P450 enzyme critical in ecdysone biosynthesis. Insect Biochem. Mol. Biol. 34: 991–1010.

Yamanaka, N., K. F. Rewitz, and M. B. O'Connor, 2013 Ecdysone control of developmental transitions: lessons from *Drosophila* research. Annu. Rev. Entomol. 58: 497–516.

Yoshiyama, T., T. Namiki, K. Mita, H. Kataoka, and R. Niwa, 2006 Neverland is an evolutionally conserved Rieske-domain protein that is essential for ecdysone synthesis and insect growth. Development 133: 2565–2574.

Yoshiyama-Yanagawa, T., S. Enya, Y. Shimada-Niwa, S. Yaguchi, Y. Haramoto *et al.*, 2011 The conserved rieske oxygenase DAF-36/Neverland is a novel cholesterol-metabolizing enzyme. J. Biol. Chem. 286: 25756–25762.

Zhang, Z., Q. Xie, T. O. Jobe, A. R. Kau, C. Wang *et al.*, 2016 Identification of AtOPT4 as a plant glutathione transporter. Mol. Plant 9: 481–484.

Communicating editor: B. Sullivan